Science Translational Medicine
AAAS

# Rapamycin Reverses Cellular Phenotypes and Enhances Mutant Protein Clearance in Hutchinson-Gilford Progeria Syndrome Cells

Kan Cao, *et al.*

*Sci Transl Med* **3**, 89ra58 (2011);
DOI: 10.1126/scitranslmed.3002346

Editor's Summary

## The Young and the Youthless

In the novel Brideshead Revisited, Evelyn Waugh reminisces about "the langor of youth" and laments "how quickly, how irrecoverably lost" is the bloom. Although every adult can relate to this cri de coeur, in no case is youth lost more swiftly or more dramatically than in children suffering from Hutchinson-Gilford progeria syndrome (HGPS), a genetic disease characterized by premature aging and death in adolescence or the teen years. In studies of the normal aging process, the versatile drug rapamycin has been shown to extend longevity in animal models. Now, Cao et al. reveal that the drug reverses disease-distinguishing defects in cells from HGPS patients. These findings raise the possibility that rapamycin might be repurposed for the treatment of this dire disease. Children with HGPS display many of the phenotypes we associate with aging: hair loss, bone deficits, hardening of the skin by 1 or 2 years of age, and heart disease and stroke often by the age of 12. The disease is caused by a point mutation in the gene that encodes the nuclear structural protein lamin A. This genetic defect creates an improperly processed version of the lamin A protein —called progerin—that accumulates in HGPS cells and wreaks havoc on cellular form and function. Several studies indicate that normal human cells also express tiny amounts of progerin, which accumulates as a person ages. Skin cells (fibroblasts) from HGPS patients display a variety of blemishes, including slowed growth, an abbreviated life span, nuclear blebbing (bulging of the nuclear membrane), and the characteristic accumulation of insoluble progerin in the cytoplasm. Protein aggregation is also a hallmark of several neurodegenerative diseases, and there is some evidence that rapamycin might be useful in the treatment of these disorders by stimulating macroautophagy—a process by which cells clear junk protein and trashed organelles. Thus, Cao et al. tested whether rapamycin also helps to rid HGPS cells of progerin build-up and to remedy the resulting cellular quirks. Indeed, HGPS cells treated with rapamycin showed enhanced progerin degradation, slowed senescence, and reduced nuclear blebbing relative to untreated cells. Mechanistic experiments in normal human fibroblasts revealed that rapamycin treatment increased clearance of soluble progerin by activating the autophagic-lysosomal pathway, which inhibited the formation of insoluble aggregates. Blocking the expression of an autophagy-related gene with small RNAs enhanced progerin accumulation. The new work has helped to form the basis for a clinical trial of the rapamycin analog everolimus in children with HGPS and may offer insights into normal aging as well. Thus, in science, as in youth —according to Waugh —new notions are continually "revealed to us in whose light all our previous knowledge must be rearranged."





*Science Translational Medicine* (print ISSN 1946-6234; online ISSN 1946-6242) is published weekly, except the last week in December, by the American Association for the Advancement of Science, 1200 New York Avenue NW, Washington, DC 20005. 

PROGERIA

# Rapamycin Reverses Cellular Phenotypes and Enhances Mutant Protein Clearance in Hutchinson-Gilford Progeria Syndrome Cells

Kan Cao,[1,2]* John J. Graziotto,[3]* Cecilia D. Blair,[1] Joseph R. Mazzulli,[3] Michael R. Erdos,[1] Dimitri Krainc,[3†] Francis S. Collins[1†]

**Hutchinson-Gilford progeria syndrome (HGPS) is a lethal genetic disorder characterized by premature aging. HGPS is most commonly caused by a de novo single-nucleotide substitution in the *lamin A/C* gene (*LMNA*) that partially activates a cryptic splice donor site in exon 11, producing an abnormal lamin A protein termed progerin. Accumulation of progerin in dividing cells adversely affects the integrity of the nuclear scaffold and leads to nuclear blebbing in cultured cells. Progerin is also produced in normal cells, increasing in abundance as senescence approaches. Here, we report the effect of rapamycin, a macrolide antibiotic that has been implicated in slowing cellular and organismal aging, on the cellular phenotypes of HGPS fibroblasts. Treatment with rapamycin abolished nuclear blebbing, delayed the onset of cellular senescence, and enhanced the degradation of progerin in HGPS cells. Rapamycin also decreased the formation of insoluble progerin aggregates and induced clearance through autophagic mechanisms in normal fibroblasts. Our findings suggest an additional mechanism for the beneficial effects of rapamycin on longevity and encourage the hypothesis that rapamycin treatment could provide clinical benefit for children with HGPS.**

## INTRODUCTION

Classic Hutchinson-Gilford progeria syndrome (HGPS) is an autosomal dominant genetic disease that is observed in about 1 in 4 million live births (*1*, *2*). Patients with HGPS appear normal at birth but begin to display alopecia, growth retardation, bone abnormalities, osteoporosis, and sclerodermatous skin by 1 year of age (*1*, *3*). HGPS patients typically die at a mean age of 12 years from myocardial infarction or cerebrovascular accident (*1*). Primary fibroblasts from HGPS patients exhibit characteristic nuclear blebbing, punctate accumulations of progerin in mitotic cytoplasm (*4*), a reduced growth rate and life span, and broad epigenetic alterations in histone methylation that predate the changes in nuclear shape (*5*–*7*).

Rapamycin is a macrolide antibiotic that has been shown to affect a number of biological pathways, including the ability to extend longevity in yeast, invertebrates, and mammals (*8*–*11*). Its major cellular target, mammalian target of rapamycin (mTOR), is a central regulator of cell growth that integrates nutrient and hormonal signals and regulates diverse cellular processes (*12*). mTOR exists in two functionally distinct complexes, mTORC1 and mTORC2, both of which control cell growth (*13*). At low (nanomolar) concentrations, rapamycin inhibits mTORC1 by directly associating with its intracellular receptor FKBP12, but longer-term exposure of the cells to higher (millimolar) doses of rapamycin reduces mTORC2 function as well (*14*). Rapamycin has been approved by the U.S. Food and Drug Administration (FDA) for a variety of clinical applications, including immunosuppression and as a potential anticancer treatment (*15*). In addition, rapamycin has been shown to be potentially beneficial in the treatment of neurodegenerative diseases through the activation of macroautophagy, a process by which the cell rids itself of unnecessary proteins and damaged organelles via the lysosomal degradation pathway (*16*–*18*). Here, we test the effects of rapamycin on HGPS cells and characterize the drug's effect on progerin accumulation.

[1]Genome Technology Branch, National Human Genome Research Institute, National Institutes of Health, Bethesda, MD 20892–8004, USA. [2]Department of Cell Biology and Molecular Genetics, University of Maryland, College Park, MD 20742, USA. [3]Department of Neurology, Massachusetts General Hospital, MassGeneral Institute for Neurodegenerative Disease, Harvard Medical School, Charlestown, MA 02129, USA.
*These authors contributed equally to this work.
†To whom correspondence should be addressed. E-mail: francis.collins@nih.gov (F.S.C.); krainc@helix.mgh.harvard.edu (D.K.)

## RESULTS

### Rapamycin rescues nuclear blebbing and postpones senescence in HGPS fibroblasts

We explored the potential effects of rapamycin on cultured fibroblasts derived from HGPS patients. First, we focused on analyzing nuclear blebbing, the phenotypic hallmark of HGPS cells. Cultured fibroblasts from three HGPS patients (HGADFN169, HGADFN155, and HGADFN167) and from four control individuals (HGFDFN168, HGFDFN320, HGFDFN319, and AG08470) were used in this study. The cells were fed with fresh minimal essential medium (MEM) containing 0.68 μM rapamycin or the same volume of vehicle [dimethyl sulfoxide (DMSO), 0.025% (v/v)] every other day for a minimal duration of 2 weeks. To evaluate the long-term effect of rapamycin, treatment continued over 100 days until cellular senescence approached. Because the results were quite consistent for all tested HGPS or control cell lines, we show only the representative data from one HGPS cell line (HGADFN167) and one control line (HGFDFN168) unless otherwise indicated.

To examine rapamycin's effects on nuclear morphology, we labeled cells with an antibody to lamin A/C and an antibody to α-tubulin, which together reveal the overall cell shape (Fig. 1A). To quantitatively judge the impact of rapamycin treatment, we scored the percentage of nuclear blebbing in a blinded fashion. At least 200 randomly selected cells were scored by fluorescence microscopy for each cell line under each condition. Consistent with a previous report (*19*), with mock

treatment, more than 30% of the HGPS nuclei exhibited abnormal blebbing, and this percentage gradually increased as the cells approached senescence in culture (Fig. 1B). In comparison with the passage-matched, mock-treated HGPS cells, the rapamycin-treated HGPS cells exhibited a significant reduction in nuclear blebbing (Fig. 1B). The improvement in nuclear blebbing appeared as early as 10 days after rapamycin treatment and was retained in the long-term experiments despite the increase in cellular age (Fig. 1B). A similar reduction of the nuclear blebbing phenotype was observed even when rapamycin treatment was started in later-passage HGPS cells (passage 15 and beyond), suggesting that the drug is capable of reversing the nuclear blebbing phenotype in HGPS cells. Rapamycin-treated normal control cells also exhibited a significant decrease in blebbing compared with their mock-treated counterparts (Fig. 1B).

Previous analysis has demonstrated that progerin accumulation induces progressive alterations in the trimethylation of Lys[27] in histone

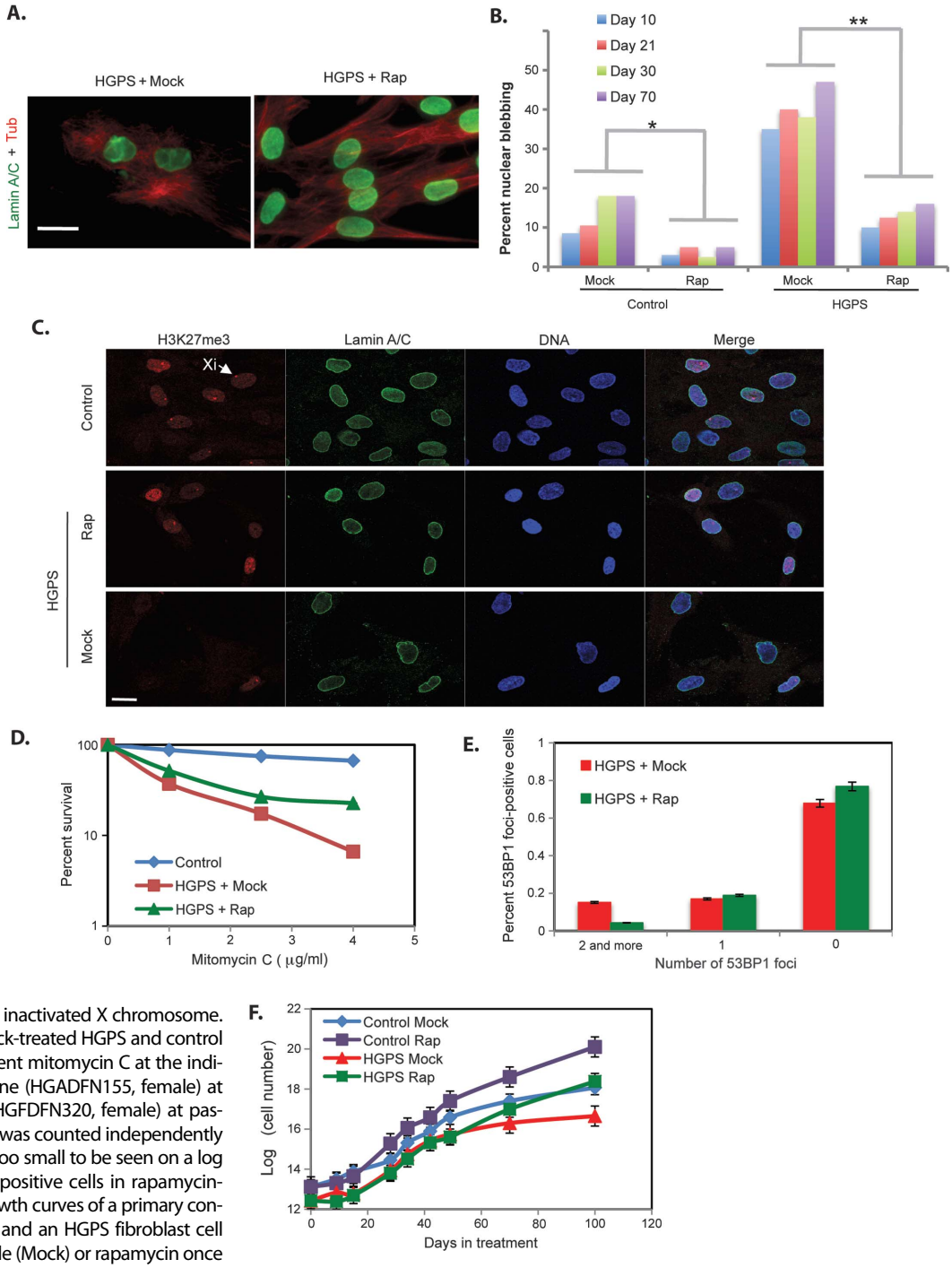


**Fig. 1.** Rapamycin rescues nuclear blebbing and postpones senescence in Hutchinson-Gilford progeria syndrome (HGPS) fibroblasts. (**A**) Immunofluorescence images of an HGPS cell line (HGADFN167) at passage 15 treated with vehicle (DMSO) or rapamycin (Rap) for 14 days. Red, anti–α-tubulin (Tub, DM1α); green, anti–lamin A/C (MAB3211). Scale bar, 20 μm. (**B**) Percentage of nuclear blebbing when HGPS (HGADFN167) and control (HGFDFN168) fibroblast cells were treated once every other day for 70 days with rapamycin (*$P$ = 0.015; **$P$ = 0.0002). These experiments were performed in three independent HGPS cell lines and in four control lines. Representative data from one HGPS cell line (HGADFN167) and one control line (HGFDFN168) are shown. Percentage of nuclear blebbing was scored by a blinded observer who viewed more than 200 randomly chosen cells. For statistical analysis, we used a two-tailed Student's $t$ test to compare the mock- and rapamycin-treated cells at four time points (days 10, 21, 30, and 70). A $P$ value of <0.05 was considered significant. (**C**) Representative immunofluorescence images of an HGPS fibroblast cell line (HGADFN155, female) at passage 10 and a control fibroblast cell line (HGFDFN320, female) at passage 10 treated with vehicle (Mock) or rapamycin for 14 days. Red, anti-H3K27me3; green: goat anti–lamin A/C (N18); blue, DAPI staining of DNA. Scale bar, 20 μm. Xi, inactivated X chromosome. (**D**) Sensitivity of rapamycin- and mock-treated HGPS and control fibroblast cells to DNA-damaging agent mitomycin C at the indicated concentration. An HGPS cell line (HGADFN155, female) at passage 12 and a control cell line (HGFDFN320, female) at passage 15 were used. Each experiment was counted independently three times, but the error bars were too small to be seen on a log scale. (**E**) Percentage of 53BP1 foci–positive cells in rapamycin- and mock-treated HGPS cells. (**F**) Growth curves of a primary control fibroblast cell line (HGFDFN168) and an HGPS fibroblast cell line (HGADFN167) treated with vehicle (Mock) or rapamycin once every 2 days for 100 days ($n$ = 3 for each condition).

H3 (H3K27me3), a mark of facultative heterochromatin (a reversible form of tightly packed, transcriptionally silent DNA) (*6*). The changes in H3K27me3 may be induced by the disruption of the nuclear scaffold and occur before changes in nuclear shape. To evaluate the potential effect of rapamycin on the epigenome, we examined the nuclear staining of H3K27me3 in rapamycin- or mock-treated female fibroblasts. In female cells, it is known that H3K27me3 normally coats the inactivated X chromosome (Xi); in HGPS cells, this H3K27me3 staining on Xi is partially lost (Fig. 1C). We found that rapamycin treatment restored the normal distribution of H3K37me3 in HGPS fibroblasts (Fig. 1C and fig. S2). In addition, because an increase in genome instability has been reported in HGPS cells (*20*, *21*), we examined whether rapamycin treatment can improve this phenotype. Using mitomycin C, a chemical that induces double-strand DNA breaks, we found that rapamycin-treated HGPS cells showed reduced sensitivity to DNA damage (Fig. 1D). Moreover, using immunofluorescence staining, we observed in rapamycin-treated cells a significant reduction in tumor protein p53-binding protein 1 (TP53BP1)–positive nuclei with multiple foci relative to control cells. TP53BP1 binds to sites of DNA damage in the nucleus (*21*). Thus, these observations indicate that rapamycin treatment helps to prevent DNA damage caused by accumulation of progerin (Fig. 1E).

We also determined the HGPS cell proliferation rate with and without rapamycin treatment by quantifying the total cell numbers during the course of treatment. Initially, we had predicted a decrease in growth rate because of rapamycin's well-characterized antiproliferative effect (*22*), which may cause the death of unhealthy cells with pronounced nuclear defects. Surprisingly, we only noticed a slight drop in cell number at the beginning of the treatment (less than 2 weeks), and no significant delay in proliferation rate was observed when rapamycin was used at the indicated concentration during the long-term treatment (Fig. 1F). Indeed, after 60 days of rapamycin treatment, when the proliferation rate in the mock-treated cells began to drop as cellular senescence approached, the cell count continued upward in both the control and the HGPS rapamycin-treated cell lines (Fig. 1F). Consistent with these findings, when senescence-associated β-galactosidase (SA-β-Gal) activity was measured at day 60 of treatment, we observed significantly fewer β-Gal–positive cells in rapamycin-treated versus mock-treated cells (fig. S2), indicating that rapamycin slowed the progression of cellular senescence. Accordingly, the maximum cellular life span was significantly extended by at least 30 days in both control and HGPS cell lines treated with rapamycin. In support of a rapamycin effect on senescence, fluorescence-activated cell sorting (FACS) analysis revealed a significant increase of S-phase cells in the context of rapamycin but not mock treatment, which suggests that a higher percentage of the rapamycin-treated cells were continuing through the cell cycle (fig. S3). We concluded that rapamycin treatment rescues nuclear phenotypes and postpones cellular senescence in HGPS and control cells.

### Rapamycin decreases progerin levels in HGPS fibroblasts

Previous studies have shown that rapamycin may promote the degradation of unnecessary or toxic components inside the cell through activation of autophagy (*23*, *24*). In cultured HGPS cells, the severity of nuclear phenotypes in later passages correlates with an apparent increase in progerin accumulation (*5*). Moreover, progerin is also produced in normal cells and increases in abundance as senescence approaches (*4*, *25*). Therefore, we hypothesized that rapamycin induces the accelerated degradation of progerin in treated HGPS and control cells. To test this hypothesis, we generated a custom antibody against progerin using a peptide located at the cryptic splicing junction as an antigen (anti-progerin). This antibody specifically recognized progerin, but not lamin A or C in Western (immuno) blotting and immunofluorescence analyses (fig. S4). When normalized with a β-actin control, quantification of protein by Western blot revealed a ~50% reduction in progerin amounts in rapamycin-treated HGPS cells on day 60 of treatment relative to mock-treated cells (Fig. 2, A and B). Quantification of the intensities of lamin A and C bands revealed that the amount of wild-type lamin A was reduced by about 25%, and the lamin C amount was not affected. To test rapamycin effectiveness, we also examined the phosphorylation state of ribosomal protein subunit S6 (rpS6, and p-rpS6 for the phosphorylated form), a target substrate in the mTOR signaling pathway (*9*), and detected the expected reduction in rpS6 phosphorylation (Fig. 2A).

To further evaluate the rapamycin-associated decrease in progerin, we used immunofluorescence microscopy to scrutinize individual HGPS cells that had been stained with anti-progerin. We consistently detected a weaker progerin staining signal in almost all of the rapamycin-treated HGPS cells (more than 1000 cells viewed from three independent HGPS cell lines), and their nuclear blebbing phenotype appeared to be substantially improved relative to mock-treated cells (Fig. 2C). Quantification confirmed the intensity reduction (Fig. 2D), consistent with the Western blotting results (Fig. 2B). We then performed quantitative reverse transcription–polymerase chain reaction (RT-PCR) assays using a pair of primers specific for progerin mRNA in rapamycin- and mock-treated HGPS and control cells. As shown in Fig. 2E, progerin mRNA expression was not down-regulated in rapamycin-treated cells, suggesting that the rapamycin effect on progerin occurs post-transcriptionally.

### Rapamycin treatment increases solubility of progerin

Having shown that rapamycin decreases progerin concentrations in HGPS cells, we next examined whether the drug alters aggregation of the protein. To this end, we used sequential extractions to examine the effect of rapamycin on solubility of progerin. Analysis of mock-treated HGPS cells revealed a significant increase in the amount of both lamin A and progerin in the SDS- and formic acid–soluble extracts compared to control cell lines (Fig. 3, A and B). This suggests that the presence of progerin results in the formation of aberrant insoluble species that also sequester lamin A and make it insoluble. Rapamycin treatment decreased the amount of insoluble lamin A and progerin in HGPS cells relative to mock-treated cells, whereas no effect was seen in control cells (Fig. 3, A and B).

We then used size exclusion chromatography (SEC) to examine Triton-soluble monomers, dimers, and potential high–molecular weight (HMW) oligomeric species of progerin and lamin A, and to investigate how the profile changes with rapamycin treatment (Fig. 3, C to F). SEC analysis of control cells indicated that lamin A eluted mainly as a 70 Å–sized species, consistent with it being a soluble dimeric intermediate that is eventually incorporated into mature lamin A polymers. The elution profile of progerin in HGPS cells revealed the presence of a HMW 83 Å–sized oligomeric species as well as a 36 Å–sized putative monomeric form (Fig. 3, D and F). After treatment of HGPS cells with rapamycin, the amounts of the 36 Å–sized progerin monomer were decreased, whereas those of the 83 Å–sized HMW species were increased. These results suggest that rapamycin promotes the formation of soluble oligomeric forms of progerin. Rapamycin treatment had minimal effect on lamin A moieties in control cells, whereas

rapamycin-treated HGPS cells showed a significant increase in a 36 Å–sized putative lamin A monomer, suggesting that the solubility of lamin A was increased with treatment (Fig. 3, D and E).

Together, these findings support the hypothesis that rapamycin diminishes the formation of insoluble progerin and promotes the solubility of lamin A and progerin in HGPS cells.

### Rapamycin promotes clearance of progerin by autophagy

To examine more directly how rapamycin may facilitate progerin clearance, we performed radiolabeled pulse-chase experiments followed by immunoprecipitation (IP) with a lamin A/C antibody in HGPS fibroblasts (Fig. 4A). These experiments revealed that the amounts of soluble progerin, but not lamin C, decreased significantly faster in rapamycin-treated compared to mock-treated HGPS fibroblasts, indicating that the progerin protein is cleared more rapidly (Fig. 4A). Rapamycin treatment shortened the half-life of progerin and increased the first-order rate constant. Rapamycin is known to increase macroautophagy (*16*–*18*); therefore, to assess whether the macroautophagy process was involved in drug-enhanced progerin clearance, we repeated the pulse-chase experiments in the presence of the lysosomal proton pump inhibitor bafilomycin A1 (Baf). Treatment of HGPS fibroblasts with Baf, which causes accumulation of autophagosomes and reduces protein clearance, significantly inhibited the effect of rapamycin, suggesting that the increased clearance of progerin observed with rapamycin treatment is mediated by the autophagic-lysosomal pathway (Fig. 4B).

To further investigate the effects of pharmacological inhibition of autophagy, we assessed the consequences of suppressing the expression of *ATG7*, an autophagy-specific gene that encodes a ubiquitin-activating enzyme (E1)–like protein required to activate the autophagy-related proteins Atg12 and Atg8 during the initial steps of autophagosome formation (*26*, *27*). Rapamycin-treated HeLa cells that had been engineered to stably express a doxycycline (DOX)–inducible green fluorescent protein (GFP)–progerin fusion protein (*6*) were transfected with a small hairpin RNA (shRNA) expression vector that encoded either *ATG7*-specific or scrambled shRNAs. The degradation of GFP-progerin was assessed 24 hours after DOX washout. In rapamycin-treated cells that expressed the *ATG7*-specific shRNA, endogenous amounts of the ATG7 protein were reduced by about 40% relative to rapamycin-treated cells that expressed the scrambled shRNA control (Fig. 4C). In addition, when compared with the scrambled shRNA control, *ATG7* knockdown resulted in a

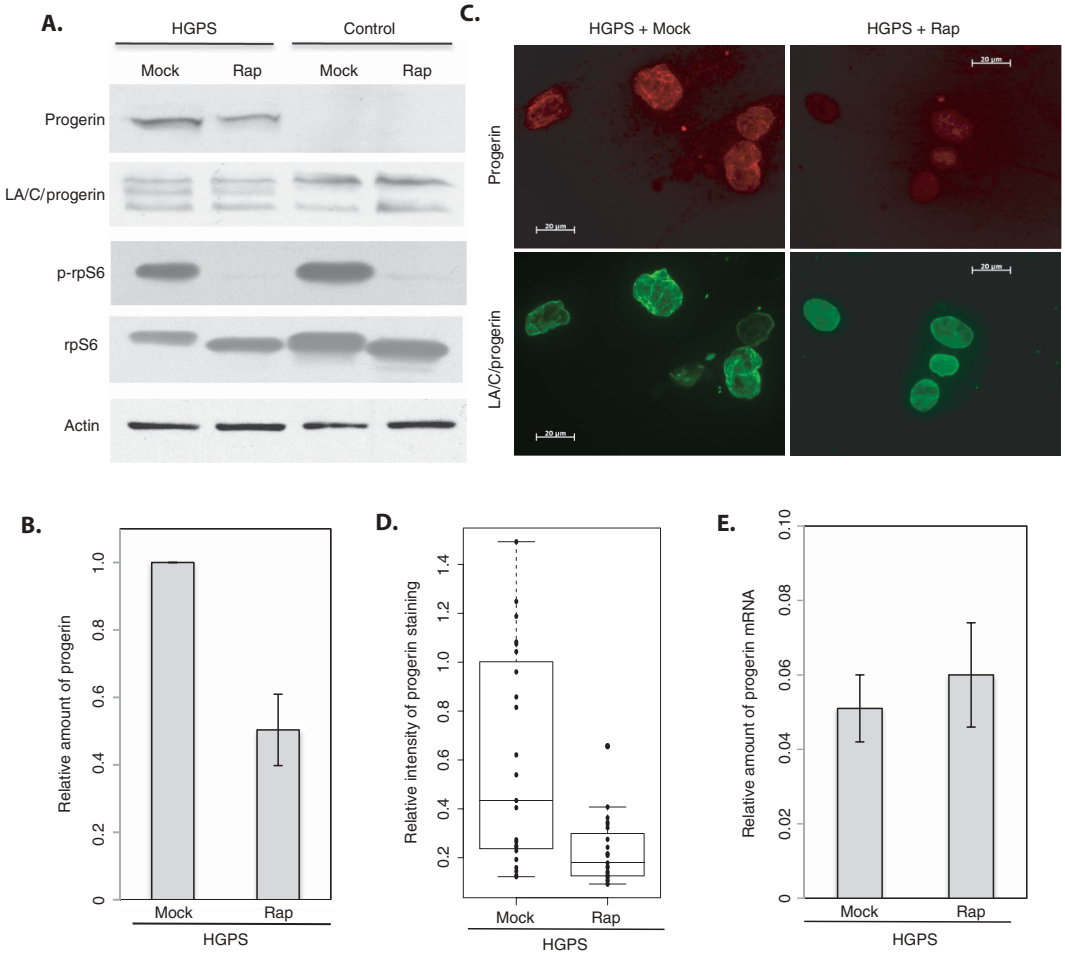


**Fig. 2.** Progerin protein concentrations are reduced in rapamycin-treated HGPS cells. (**A**) Western (immuno) blotting analysis of relative progerin amounts in rapamycin- and mock-treated HGPS cells. Antibodies used are shown at the left. A custom anti-progerin antibody was used to detect progerin, and a mouse anti–lamin A/C antibody (LA/C/progerin, MAB3211) was used to detect wild-type lamin A and lamin C. The effect of rapamycin on inhibition of the mTOR pathway was evaluated by immunoblotting assay with antibodies to unphosphorylated ribosomal subunit protein S6 (rpS6) and its phosphorylated counterpart (p-rpS6). β-Actin (Actin) was used as a loading control. (**B**) Quantification of the progerin band intensity in rapamycin- and mock-treated HGPS samples shown in (A). The relative progerin intensity was normalized using actin as an internal control and quantified as described (*7*). (**C**) Immunofluorescence images (exposure time–matched) of an HGPS cell line (HGADFN167) at passage 15, mock-treated or treated with rapamycin for 60 days. (**D**) Box plot analysis of the relative progerin staining intensity in HGPS fibroblasts stained with an anti-progerin antibody and counterstained with a mouse anti–lamin A/C antibody (MAB3211) ($n = 23$ for both samples; $P = 0.0005$). (**E**) Quantitative RT-PCR analysis of total progerin mRNA in rapamycin- or mock-treated HGPS fibroblast cells with progerin-specific primers. The relative expression values for progerin were normalized to the mean values of endogenous actin.

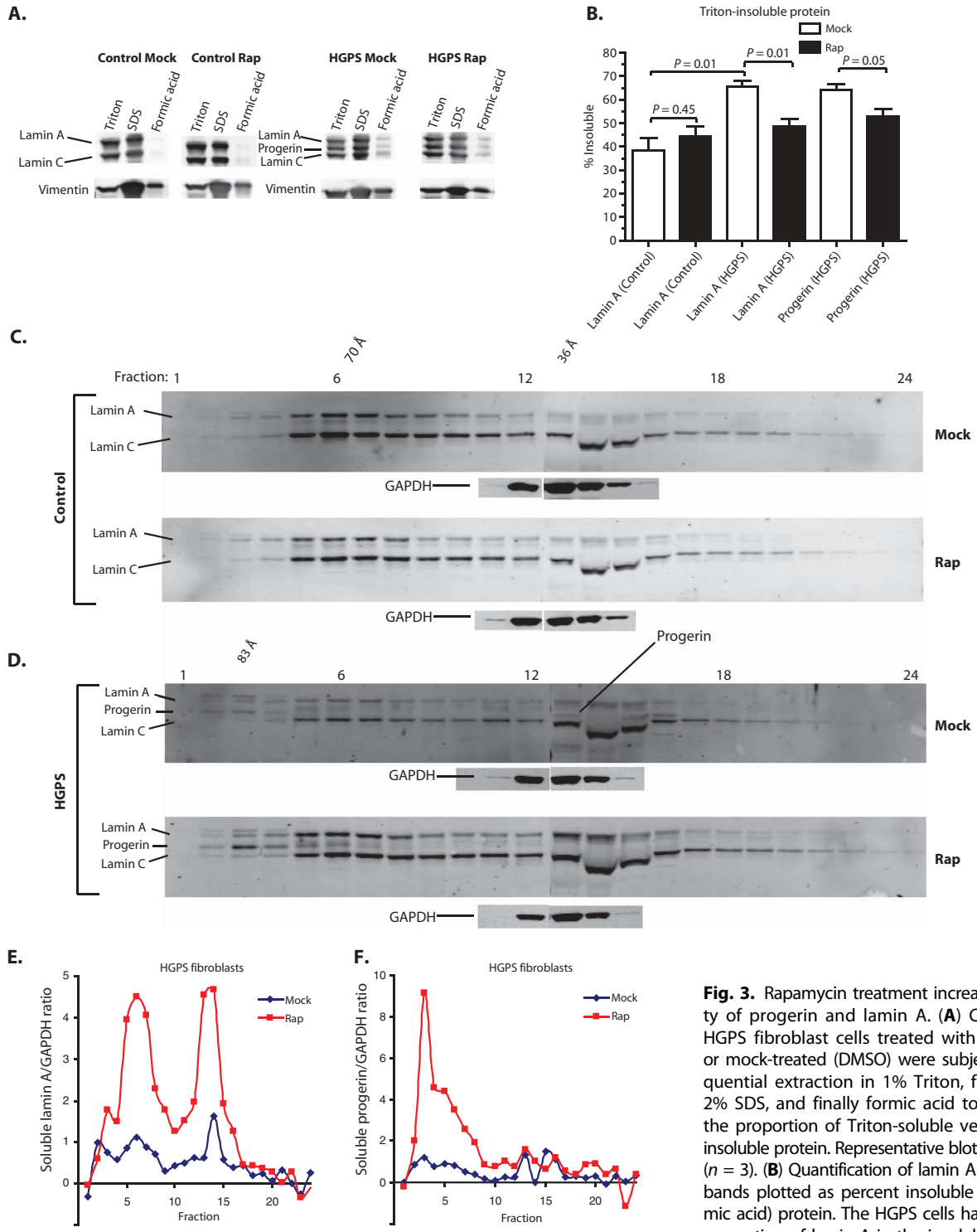


**Fig. 3.** Rapamycin treatment increases solubility of progerin and lamin A. (**A**) Control and HGPS fibroblast cells treated with rapamycin or mock-treated (DMSO) were subjected to sequential extraction in 1% Triton, followed by 2% SDS, and finally formic acid to determine the proportion of Triton-soluble versus Triton-insoluble protein. Representative blots are shown ($n$ = 3). (**B**) Quantification of lamin A or progerin bands plotted as percent insoluble (SDS + formic acid) protein. The HGPS cells have a higher proportion of lamin A in the insoluble fractions compared to control. Rapamycin restored the solubility of lamin A and increased the solubility of progerin as well ($n$ = 3, mean ± SEM). (**C** and **D**) Triton-soluble protein extracts from (C) control or (D) HGPS fibroblasts treated with DMSO (Mock) or rapamycin were subjected to SEC and separated into 24 fractions, which were analyzed by SDS-PAGE and immunoblotting. Blots were probed with anti–lamin A/C antibody. Signals were quantified using a Li-Cor Odyssey and normalized to glyceraldehyde-3-phosphate dehydrogenase (GAPDH). (**E** and **F**) Although no major changes were seen between treatments in control fibroblasts, both lamin A (E) and progerin (F) showed increased solubility in HGPS fibroblasts when treated with rapamycin compared to mock treatment. Monomeric progerin (36 Å) was decreased in HGPS cells upon rapamycin treatment, whereas high–molecular weight (HMW) (83 Å) progerin was increased (D). Representative blots are shown.

significant accumulation of GFP-progerin in rapamycin-treated cells, further suggesting that macroautophagy plays a role in progerin clearance (Fig. 4C).

As a final test of the effect of autophagy in the rapamycin-induced clearance of progerin, we treated the GFP-progerin–expressing HeLa cells with 3-methyladenine (3-MA), an inhibitor of phosphoinositide 3-kinase, which is essential for induction of autophagy (*28*). 3-MA significantly reduced the decay rate of progerin in the presence of rapamycin (Fig. 4D).

Protein ubiquitination has recently emerged as an important signal for selective autophagic clearance and involves autophagy adaptor proteins that bind both ubiquitinated cargo and autophagosomes (*29*–*31*). Distinct effects have been described for the various types of polyubiquitin chains that are attached to proteins destined for clearance. Polyubiquitin chains that are linked via their lysine residue 63 (K63-linked polyubiquitin chains) promote autophagic clearance of oligomeric and aggregated proteins (*31*, *32*). To examine whether progerin destined for degradation is ubiquitinated, we transfected HeLa cells

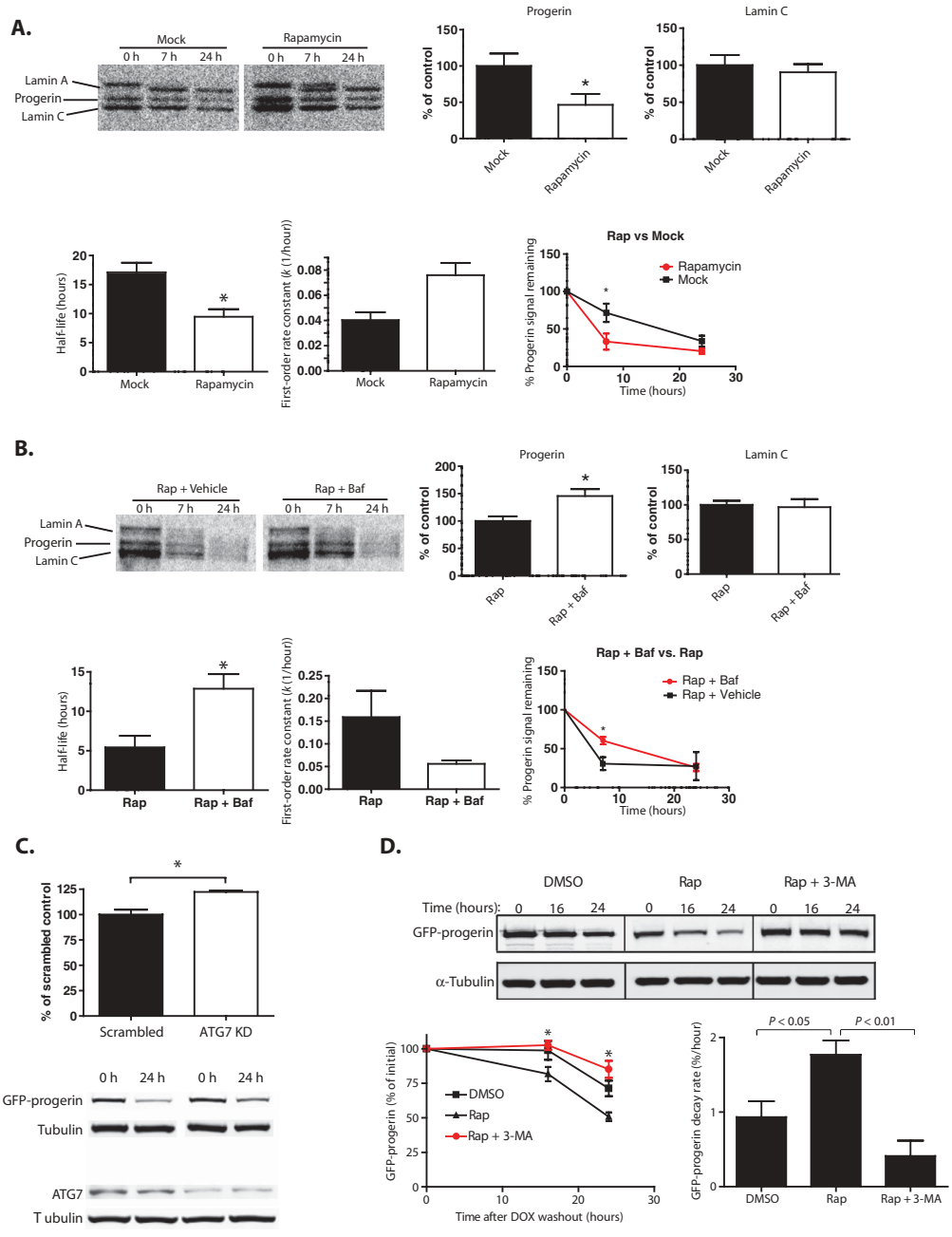


**Fig. 4.** Rapamycin promotes clearance of progerin by autophagy. (**A**) Radiolabeled pulse-chase experiments in mock- and rapamycin-treated HGPS fibroblasts were followed by immunoprecipitation with a mouse anti–lamin A/C antibody (MAB3211). Relative to mock-treated cells, the rapamycin-treated cells displayed a shorter half-life for progerin and an increase in the progerin degradation–associated rate constant, indicating faster clearance of progerin in the presence of the drug. (**B**) The pulse-chase experiments in (A) were repeated in the presence of Baf. The rapamycin-associated increase in progerin clearance was inhibited in Baf-treated relative to untreated cells, suggesting that the observed effect was mediated by autophagy. Data for the histograms in (A) and (B) were evaluated 7 hours after initiation of the chase (mean ± SEM, $n = 3$; *$P < 0.05$). (**C**) Rapamycin-treated, cultured HeLa cells that had been engineered to express a doxycycline (DOX)–inducible green fluorescent protein–progerin fusion protein (GFP-progerin) (*6*) were transfected with an *ATG7*-knockdown (KD) vector that expressed either *ATG7*-specific or scrambled shRNAs, and progerin degradation was assessed 24 hours after DOX washout. In cells that expressed the *ATG7*-knockdown construct, ATG7 expression was decreased by ~40% compared to those that expressed the scrambled control. In cells that were treated with the *ATG7*-specific shRNA expression vector, 22% more progerin remained 24 hours after DOX washout compared to the scrambled control construct ($n = 3$, $P = 0.01$). (**D**) Cells that expressed GFP-progerin were treated with DMSO, rapamycin, or rapamycin plus 3-MA, and the degradation of progerin was tracked by GFP Western (immuno) blotting with rabbit anti-GFP (Sigma) after DOX washout. Mouse anti–α-tubulin (DM1α) was used as a loading control. Rapamycin treatment increased the decay rate of progerin compared to DMSO-treated cells, and this effect was blocked by the addition of 3-MA ($n = 3$; DMSO compared to rapamycin, $P = 0.0429$; rapamycin compared to rapamycin + 3-MA, $P = 0.0084$).

that expressed GFP-progerin with either an expression vector that encoded hemagglutinin (HA)–tagged ubiquitin (capable of producing polyubiquitin chains) or one that encoded HA-tagged K63-ubiquitin (capable of producing only K63-linked polyubiquitin chains). The progerin fusion protein was preferentially ubiquitinated by K63-linked polyubiquitin, which suggests that progerin is a substrate for autophagic clearance (Fig. 5A). This conclusion was further supported by our finding that progerin interacts with p62, an autophagy adaptor protein that represents a functional link between ubiquitinated cargos and autophagosomes (*33*). Indeed, p62 was coimmunoprecipitated with progerin from GFP-progerin–producing HeLa cells, and additional treatment of such cells with Baf increased the amount of p62 that precipitated with progerin, further indicating that progerin is a substrate for autophagic clearance (Fig. 5B). Furthermore, we detected the p62-progerin

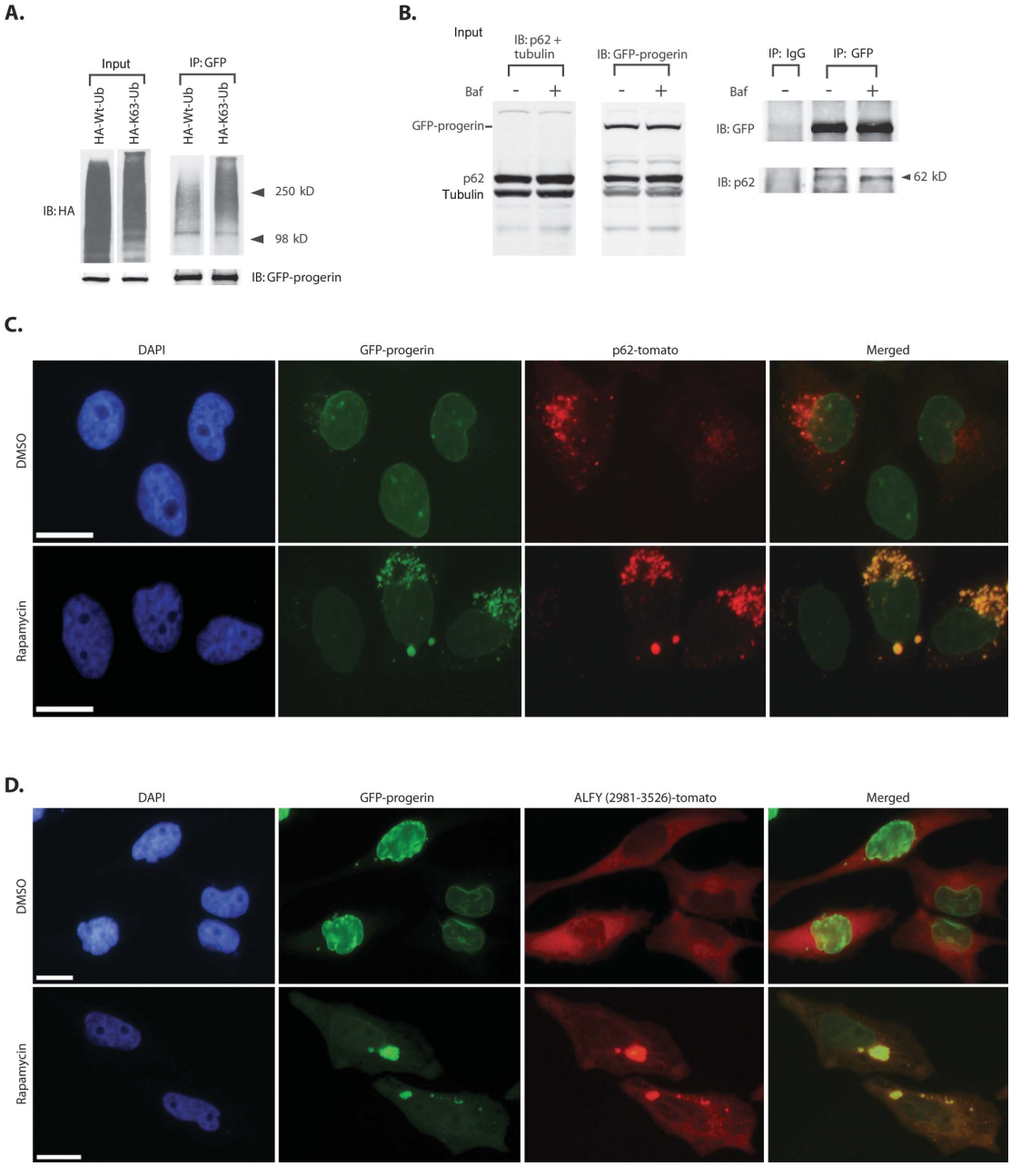


**Fig. 5.** Progerin interacts with autophagy-related proteins. (**A**) Progerin is modified by K63-linked polyubiquitin. GFP-progerin–expressing HeLa cells were transfected with either HA-tagged wild-type ubiquitin (HA-Wt-Ub) or HA-K63-Ub. The cells were harvested, lysed, and subjected to Western (immuno) blotting. The Western blots were probed for the HA tag with an antibody to HA (mouse anti-HA) and for GFP expression using rabbit anti-GFP (Sigma). When immunoprecipitated (IP) from cell lysates with rabbit anti-GFP (Invitrogen), progerin was shown to be preferentially ubiquitinated by K63-linked ubiquitin. A representative immunoblot (IB) is shown ($n = 3$). (**B**) Co-IP of p62 and progerin. GFP-progerin–expressing HeLa cells were either mock-treated or treated with 200 nM Baf for 6 hours and lysed in co-IP buffer. Equivalent amounts of protein were immunoprecipitated from the lysate with rabbit anti-GFP (Invitrogen) overnight at 4°C. Input and IPs were subjected to Western blotting, and the blots were probed for mouse anti-p62 and mouse anti-tubulin (DM1$\alpha$) simultaneously and sequentially probed for GFP-progerin with rabbit anti-GFP (Sigma). p62 coimmunoprecipitated with progerin, and Baf treatment increased the amount of the p62-progerin complex isolated by co-IP. The experiment was performed twice ($n = 2$), and a representative immunoblot is shown. (**C**) Colocalization of p62 and progerin. Stably transfected GFP-progerin–expressing HeLa cells were treated with DMSO or rapamycin and then transfected with a p62-tomato expression vector. Cells were fixed 4 days later and visualized by fluorescence microscopy. (**D**) Colocalization of C-terminal ALFY-tomato protein with progerin in HeLa cells. HeLa cells that stably express GFP-progerin were cultured with either DMSO or 0.68 μM rapamycin for 15 days. The cells were then transfected with an N-terminal ALFY (1–1278) expression vector and incubated for 3 hours with 50 nM Baf just before fixation to enhance the detection of putative autophagic substrates. Increased colocalization of ALFY with progerin was observed after rapamycin treatment. Baf was added before fixation to enhance the visualization of autophagic substrates in (C) and (D). Scale bars, 10 μm for each image.

interaction in GFP-progerin–producing HeLa cells that had been transfected with the pDEST-tdTomato-p62 expression vector (*34*), which encodes p62 fused to the fluorescent tdTomato molecule (p62-tomato). Cells were treated with Baf before fixation to facilitate the visualization of autophagic structures. Colocalization of the p62-tomato and GFP-progerin proteins was increased in cells treated with rapamycin compared to mock (DMSO)–treated control cells (Fig. 5C). These results suggest that p62 provides a molecular link between ubiquitination of accumulated progerin and its degradation by autophagy. Finally, we demonstrated the colocalization of progerin with the zinc finger protein autophagy-linked FYVE (ALFY), which functions in conjunction with p62 and preferentially affects the clearance of aggregation-prone proteins (*35*). In cells transfected with C-terminal ALFY-tomato expression vector (Fig. 5D), increased colocalization of progerin with ALFY was observed in the presence of rapamycin relative to control cells. Similar results were obtained with an N-terminal ALFY-tomato construct (fig. S5). Similar to p62 colocalization, the colocalization of ALFY and progerin occurred in a juxtanuclear position within the cytosol, further suggesting that these proteins target progerin for autophagic clearance.

## DISCUSSION

In summary, we have shown that rapamycin abolishes characteristic nuclear defects, markedly prolongs cellular life span, and enhances the turnover of progerin in cultured HGPS fibroblasts. Rapamycin decreased the formation of insoluble progerin aggregates and promoted clearance of soluble progerin by autophagy. This observation is in agreement with another study in polyglutamine disease models wherein the effect of rapamycin was most pronounced before aggregate formation; this observation suggests that the drug enhances clearance of monomeric and oligomeric toxic species rather than large aggregates (*36*).

The results reported herein support rapamycin as a potential treatment for children with HGPS. Now under consideration is a clinical trial in such patients of the drug everolimus, a rapamycin analog that has proven to be relatively safe in children (*37*). It is possible that other laminopathies could benefit from the same rapamycin-related treatment strategy. Furthermore, the findings described herein may have consequences for an understanding of the normal process of aging. Several recent studies report that the progerin protein is expressed at low amounts in normal individuals but accumulates with age (*4*, *25*, *38*). Rapamycin has been shown to prolong life span in normal mice (*9*). Thus, it is possible that the same mechanism of accelerating the clearance of toxic progerin complexes contributes to rapamycin's beneficial effect on longevity.

## MATERIALS AND METHODS

### Cell culture and rapamycin treatment

Primary human dermal fibroblasts were cultured in MEM (Invitrogen/Gibco) supplemented with 15% fetal bovine serum (FBS) (Invitrogen) and 2 mM L-glutamine. The primary fibroblast cell lines used in our studies were AG08470 (control) (ordered from Coriell Cell Repositories) and HGADFN167 (HGPS), HGADFN169 (HGPS), HGADFN155 (HGPS), HGFDFN168 (control), HGFDFN319 (control), and HGFDFN320 (control) from Progeria Research Foundation. For consistency, all results in this report correspond to fibroblasts from HGADFN167 (HGPS) and HGFDFN168 (control) unless otherwise indicated. Control and HGPS fibroblasts were replenished with fresh MEM containing 0.68 μM rapamycin (Sigma) every other day for up to 150 days.

### Antibodies

The antibodies used in the study included a rabbit polyclonal antibody to a peptide from progerin (CKKSASGSGAQSPQN-amide), which was used by YenZym to generate a custom peptide antibody (anti-progerin), a mouse anti–lamin A/C antibody (MAB3211, Chemicon), a rabbit anti–lamin A/C antibody (Santa Cruz), a goat anti–lamin A/C (N18, Santa Cruz), a mouse anti-H3K27me3 antibody (Abcam), rabbit anti–p-rpS6 (specific for the phosphorylated form of rpS6 on $Ser^{240/244}$) and anti-rpS6 antibodies (Cell Signaling), a rabbit anti-53BP1 antibody (Abcam), a horseradish peroxidase (HRP)–conjugated anti-actin antibody (Sigma), a mouse anti-tubulin antibody (DM1α, Sigma), a mouse anti-p62 antibody (BD Biosciences), a rabbit anti-ATG7 antibody (Abgent), two rabbit anti-GFP antibodies (Invitrogen and Sigma G1544), a mouse anti-vimentin antibody (BD Biosciences), a mouse anti-HA antibody (Cell Signaling, clone 6E2), Alexa 488– or Alexa 594–conjugated donkey anti-rabbit or donkey anti-mouse immunoglobulin G (IgG) antibodies (Molecular Probes), and a mouse anti-GAPDH (glyceraldehyde-3-phosphate dehydrogenase) antibody (Abcam).

### Quantitative RT-PCR and data analysis

Quantitative RT-PCR was performed to measure the expression levels of progerin, lamin A, and β-actin. All reactions were carried out at least in triplicate on an Applied Biosystems 7900HT Fast Real-Time PCR System with SYBR Green mix (Qiagen) according to the manufacturer's instructions. Reaction conditions were as follows: 2 min at 50°C, 1 cycle; 10 min at 95°C, 1 cycle; 15 s at 95°C, 15 s at 58°C, 30 s at 72°C, 40 cycles. Primers for β-actin were obtained from Ambion (Applied Biosystems Inc.). For amplifying progerin mRNA, the sequence of the forward PCR primer was 5′-GCAACAAGTCCAATGAGGACCA-3′ and for the reverse primer was 5′-CATGATGCTGCAGTTCTGGGGGCTCTGGAC-3′. To normalize for mRNA input in each reaction, we calculated the relative expression values for progerin by normalizing progerin mRNA levels to endogenous β-actin RNA levels in each sample. Expression values for each gene were expressed as means ± SD of the experimental triplicates.

### Immunofluorescence and quantitative analysis

Human primary skin fibroblasts grown on chamber slides (Nunc) were fixed with 4% formaldehyde in phosphate-buffered saline (PBS) for 20 min at room temperature followed by a 5-min treatment with 0.5% Triton X-100 in PBS. The fixed cells were rinsed with PBS and blocked with 10% horse serum and 4% bovine serum albumin (BSA) in PBS for 30 min. Cells were then incubated for 3 hours with the primary antibodies diluted in blocking solution. The secondary antibodies were Alexa 488– or Alexa 594–conjugated donkey anti-rabbit or donkey anti-mouse IgG antibodies (Molecular Probes). All samples were also counterstained with 4′,6-diamidino-2-phenylindole (DAPI) (Vector Laboratories). Cells were observed with a LSM510 confocal microscope (Zeiss) or an Axioplan fluorescence microscope (Zeiss).

To measure the progerin staining intensity, we acquired confocal images at room temperature using a Zeiss LSM 510 NLO Meta system mounted on a Zeiss Axiovert 200M microscope with an oil immersion

Plan-Apochromat 63×/1.4 differential interference contrast objective lens. All pinholes were set with a range from 1.21 to 1.39 Airy units, which correspond to an optical slice of 1.0 μm (excluding the DAPI channel in which a multiphoton laser was used). All confocal images were of frame size 512 by 512 pixels, acquired a scan zoom setting of 2, and were line-averaged eight times. Confocal images were post-processed with the Media Cybernetics Image-Pro Plus v6.3 software package. Measurements included nucleus area ($\mu m^2$) and fluorescent intensity (minimum, maximum, mean, SD, and sum). The nuclei outlines were obtained with the DAPI staining as a template, then propagating that outline throughout the fluorescein isothiocyanate (FITC) (progerin staining) and Spectrum Orange channels (lamin A/C staining). At least 20 to 30 randomly chosen nuclei were processed per sample. The relative progerin intensity was achieved by normalizing the intensity of progerin staining (FITC) to the intensity of the lamin A/C staining (Orange).

### Mitomycin C treatment

Rapamycin- or mock-treated HGPS fibroblast cells and untreated control fibroblasts [HGADFN155 (HGPS), HGFDFN168 (control)] were seeded on six-well plates at a density of 50,000 cells per well the night before treatment. The next day, cells were washed with PBS and then incubated in serum-free MEM containing mitomycin C (0, 1, 2.5, or 4 μg/ml) (Sigma) at 37°C for 1 hour. Then, the cells were washed with regular MEM to remove mitomycin C and scored for percentage of survival with a trypan blue exclusion test of cell viability (Invitrogen) 72 hours later.

### Radiolabeled pulse-chase experiments

HGPS fibroblasts and control fibroblasts were plated in six-well dishes. Cells were rinsed once with PBS, incubated for 30 min in methionine- and cysteine-free Dulbecco's modified Eagle's medium (DMEM), and then incubated for 30 min with $^{35}$S-labeled methionine/cysteine (200 μCi/ml) in methionine- and cysteine-free DMEM ("pulsed") to label nascent proteins. Labeling was then immediately stopped by addition of "chase" medium (complete DMEM supplemented with 5 mM cysteine and 5 mM methionine). Cells were washed three times in chase medium and incubated in the chase medium for the indicated chase times. For time point collection, cells were washed in PBS and lysed in Triton lysis buffer [50 mM tris-HCl (pH 7.4), 150 mM NaCl, 5 mM EDTA, 1% Triton X-100, and a protease inhibitor cocktail] with four freeze-thaw cycles. Cleared lysates were assayed for protein content, and equivalent amounts of protein were incubated overnight with mouse anti–lamin A/C antibody [MAB3211, 1:50 (v/v) dilution] at 4°C. Protein A/G–agarose beads were added to the antibody-protein mixture, and samples were incubated for 3 more hours at 4°C. The beads were isolated and washed three times with lysis buffer, and protein was removed from the beads with 1× SDS–polyacrylamide gel electrophoresis (SDS-PAGE) protein loading buffer. The protein samples were then subjected to electrophoresis on 4 to 12% bis-tris polyacrylamide gels, and the gels were dried and exposed to a Storage Phosphor screen. The screen was scanned with a Typhoon PhosphorImager. The first-order rate constant ($k$) of progerin clearance was obtained by an exponential decay fit, and half-life was obtained with the equation Prog $t_{1/2} = \ln(2)/k$.

### Ubiquitination assays

GFP-progerin–expressing HeLa cells were transfected with 1 μg of either pRK5-HA-ubiquitin-WT or pRK5-HA-ubiquitin-K63 (Addgene). After incubation at 37°C for 24 hours, the cells were subjected to mild proteasome inhibition by incubation at 37°C with 2.5 μM MG132 for an additional 24 hours, harvested, and lysed in IP buffer (50 mM Hepes, 250 mM NaCl, 5 mM EDTA, 0.1% NP-40, pH 8) containing 10 μM MG132, ubiquitin aldehyde (0.1 μg/ml), 10 mM *N*-ethylmaleimide, and a protease inhibitor cocktail. The protein concentration in the clarified lysates was measured with the micro-BCA protein assay kit (Thermo) according to the manufacturer's instructions. Equal amounts of protein were incubated with rabbit anti-GFP [Invitrogen, 1:100 (v/v) dilution] overnight at 4°C. Protein A/G–agarose beads were added to the antibody-protein mixture, which was then incubated for an additional 3 hours at 4°C. The beads were washed as described above, and protein was isolated with 1× protein SDS-PAGE loading buffer. The protein samples were then subjected to electrophoresis on 4 to 12% bis-tris polyacrylamide gels, transferred overnight onto nitrocellulose membranes, and subjected to Western blotting with mouse anti-HA [Cell Signaling, 1:1000 (v/v) dilution] and rabbit anti-GFP [Sigma G1544, 1:2000 (v/v) dilution].

### Co-IP of p62 and GFP-progerin

GFP-progerin–expressing HeLa cells were either mock-treated or treated with 200 nM Baf (EMD Biosciences) for 6 hours and lysed in co-IP buffer [50 mM Hepes (pH 7.5), 150 mM NaCl, 1 mM EDTA, 1 mM EGTA, 1% Triton X-100, 10% glycerol, 25 mM NaF, 10 μM ZnCl, and protease inhibitor cocktail]. Equivalent amounts of protein were immunoprecipitated from the lysate with rabbit anti-GFP [Invitrogen, 1:100 (v/v) dilution] overnight at 4°C. Protein A/G–agarose beads were added to the antibody-protein mixture, which was then incubated for an additional 3 hours at 4°C. The beads were washed as described above, and protein was isolated with 1× protein SDS-PAGE loading buffer. Eluted precipitates were subjected to electrophoresis on 12% tris-glycine gels, transferred to polyvinylidene difluoride (PVDF) membranes overnight, and probed with mouse anti-p62 [BD Transduction Laboratories, 1:500 (v/v) dilution] and rabbit anti-GFP (Sigma, G1544).

### Inhibition of macroautophagy in GFP-progerin–expressing HeLa cells

The pLKO.1 ATG7 shRNA knockdown construct was obtained from Open Biosystems. HeLa cells that stably expressed a DOX-inducible GFP-progerin construct (tet-on) were transfected with an shRNA expression vector (1 μg) that encoded either an shRNA that blocks *ATG7* expression or a scrambled shRNA control and incubated in DMEM with 5% FBS for 48 hours at 37°C in the presence of DOX (2 μg/ml). Forty-eight hours after transfection, cells were washed three times with fresh medium to remove the DOX and harvested at 0 and 24 hours after DOX washout for assessment of progerin degradation.

The stably transfected HeLa cells were also treated for 4 days with 1 mM 3-MA (dissolved directly in the culture media) in the presence of DOX (2 μg/ml) and either 0.68 μM rapamycin or DMSO (control). DOX was washed out on day 4 of 3-MA treatment, and cells were harvested at 0, 16, and 24 hours after DOX washout. GFP-progerin amounts were measured in cell lysates by Western blot analysis (mouse anti-tubulin, DM1α, was used as a loading control) with a rabbit anti-GFP antibody (Sigma) followed by detection with anti-mouse or anti-rabbit IgG conjugated to either IRDye 680 or IRDye 800 (1:10,000, Li-Cor Biosciences). GFP-progerin concentrations were analyzed by densitometry and normalized to α-tubulin. Clearance rates were obtained by plotting the intensity of the normalized GFP-progerin

signal over 24 hours. These experiments were repeated three times for each condition. A two-tailed unpaired Student's *t* test was used for statistical analysis, and $P < 0.05$ was considered significant.

### Assessment of progerin colocalization with p62 and ALFY

HeLa cells that stably express inducible GFP-progerin were cultured with DOX and either DMSO or 0.68 μM rapamycin for 15 days (with a change of media every 48 hours) and then passed onto glass coverslips. The cells were then transfected, using Lipofectamine 2000 (Invitrogen), with a pDEST-tdTomato-p62 expression vector (*34*), which encoded p62 fused to the fluorescent tdTomato molecule, a pDEST–tdTomato–N-terminal ALFY (1–1278) expression vector, or a pDEST–tdTomato–C-terminal ALFY (2981–3526) expression vector (*35*), and incubated for 3 hours with 50 nM Baf (EMD Biosciences) just before fixation to enhance the detection of putative autophagic substrates. Cells were then fixed in 4% paraformaldehyde, and the cell-laden coverslips were mounted onto glass slides with 10 μl of DAPI-containing Fluoromount-G (Southern Biotech, #0100-20) and visualized on an Olympus BX50 fluorescence microscope (U-ULS100HG fluorescence observation attachment) with the 40× objective. Images were captured with an Olympus DP70 camera at equal exposures with DP controller software (Olympus, V 2.2.1.195). Cell images were imported into Photoshop CS4 (Adobe Systems) and merged, and colocalization of autophagic proteins with progerin was assessed. Three separate coverslips per condition were analyzed, with about 100 to 200 cells per coverslip. Representative images are presented in Fig. 5D and fig. S5.

### Gel filtration high-performance liquid chromatography

For SEC analysis, Triton X-100–soluble protein (400 μg) from rapamycin- or DMSO-treated fibroblasts in a total volume of 250 μl was loaded onto a Superdex 200 HR10/300 column (GE Healthcare) with an Agilent 1200 series HPLC (high-performance liquid chromatography) system. The mobile phase used to resolve the protein lysates contained 25 mM Hepes and 150 mM NaCl (pH 7.25). The fractions were collected and concentrated with Amicon Ultracel filters (Millipore) (10,000 molecular weight cutoff). Fractions (*24*) were collected, concentrated, and loaded on 4 to 12% SDS-polyacrylamide gels for immunoblot analysis with mouse anti–lamin A/C (MAB3211) and mouse anti-GAPDH.

### Sequential extraction

Fibroblasts grown on 60-mm dishes were treated with 0.68 μM rapamycin or DMSO, pelleted, weighed, and lysed with 10 μl of Triton lysis buffer per milligram of cell pellet [50 mM tris-HCl (pH 7.4), 150 mM NaCl, 1% Triton X-100, 5 mM EDTA, and protease inhibitor cocktail (11836170001, Roche)].

Cell pellets were completely resuspended in lysis buffer and subjected to four consecutive freeze-thaw cycles of 2 min each (−80°C ethanol bath/37°C water bath). The Triton X-100–soluble fraction was isolated by centrifugation at 21,000*g* for 30 min at 4°C. The resulting Triton-insoluble pellets were further extracted by the addition of SDS lysis buffer [2% SDS, 50 mM tris (pH 7.4), protease inhibitor cocktail], sonicated with three 5-s pulses, and then boiled for 20 min. These samples were then subjected to centrifugation for 20 min at 21,000*g* (25°C) to obtain the SDS-soluble fractions. The remaining SDS-insoluble pellets were finally solubilized in 70% formic acid, concentrated with a Savant SpeedVac concentrator, and washed four times with water before resuspending directly in gel-loading buffer. The samples were then subjected to SDS-PAGE. A Western blot was performed with rabbit anti–lamin A/C [Santa Cruz, 1:400 (v/v) dilution] and mouse anti-vimentin [BD Biosciences, 1:500 (v/v) dilution].

## SUPPLEMENTARY MATERIAL

www.sciencetranslationalmedicine.org/cgi/content/full/3/89/89ra58/DC1

Fig. S1. Box plot analysis of the relative H3K27me3 staining intensity in the mock- and rapamycin-treated HGPS (HGADFN155, female) and untreated control (HGFDFN320, female) cells in Fig. 1C ($n$ = 30, 41, and 41 for control, HGPS + Rap, and HGPS + Mock, respectively) ($^{*}P = 0.48$; $^{**}P = 9.5 \times 10^{-10}$).

Fig. S2. Photographs of control and HGPS fibroblasts stained for SA-β-Gal activity at day 60 with the indicated treatment.

Fig. S3. FACS cell cycle analysis of a primary control fibroblast cell line (HGADFN168) and an HGPS fibroblast cell line (HGADFN167) treated with vehicle (DMSO) or rapamycin for 60 days.

Fig. S4. Characterization of anti-progerin antibody.

Fig. S5. Progerin interacts with N-terminal ALFY.

Table S1. Cell lines used in this study.

## REFERENCES AND NOTES


1. B. C. Capell, F. S. Collins, Human laminopathies: Nuclei gone genetically awry. *Nat. Rev. Genet.* **7**, 940–952 (2006).
2. B. Korf, Hutchinson–Gilford progeria syndrome, aging, and the nuclear lamina. *N. Engl. J. Med.* **358**, 552–555 (2008).
3. M. A. Merideth, L. B. Gordon, S. Clauss, V. Sachdev, A. C. Smith, M. B. Perry, C. C. Brewer, C. Zalewski, H. J. Kim, B. Solomon, B. P. Brooks, L. H. Gerber, M. L. Turner, D. L. Domingo, T. C. Hart, J. Graf, J. C. Reynolds, A. Gropman, J. A. Yanovski, M. Gerhard-Herman, F. S. Collins, E. G. Nabel, R. O. Cannon III, W. A. Gahl, W. J. Introne, Phenotype and course of Hutchinson–Gilford progeria syndrome. *N. Engl. J. Med.* **358**, 592–604 (2008).
4. K. Cao, B. C. Capell, M. R. Erdos, K. Djabali, F. S. Collins, A lamin A protein isoform overexpressed in Hutchinson–Gilford progeria syndrome interferes with mitosis in progeria and normal cells. *Proc. Natl. Acad. Sci. U.S.A.* **104**, 4949–4954 (2007).
5. R. D. Goldman, D. K. Shumaker, M. R. Erdos, M. Eriksson, A. E. Goldman, L. B. Gordon, Y. Gruenbaum, S. Khuon, M. Mendez, R. Varga, F. S. Collins, Accumulation of mutant lamin A causes progressive changes in nuclear architecture in Hutchinson–Gilford progeria syndrome. *Proc. Natl. Acad. Sci. U.S.A.* **101**, 8963–8968 (2004).
6. D. K. Shumaker, T. Dechat, A. Kohlmaier, S. A. Adam, M. R. Bozovsky, M. R. Erdos, M. Eriksson, A. E. Goldman, S. Khuon, F. S. Collins, T. Jenuwein, R. D. Goldman, Mutant nuclear lamin A leads to progressive alterations of epigenetic control in premature aging. *Proc. Natl. Acad. Sci. U.S.A.* **103**, 8703–8708 (2006).
7. B. C. Capell, M. Olive, M. R. Erdos, K. Cao, D. A. Faddah, U. L. Tavarez, K. N. Conneely, X. Qu, H. San, S. K. Ganesh, X. Chen, H. Avallone, F. D. Kolodgie, R. Virmani, E. G. Nabel, F. S. Collins, A farnesyltransferase inhibitor prevents both the onset and late progression of cardiovascular disease in a progeria mouse model. *Proc. Natl. Acad. Sci. U.S.A.* **105**, 15902–15907 (2008).
8. R. W. Powers III, M. Kaeberlein, S. D. Caldwell, B. K. Kennedy, S. Fields, Extension of chronological life span in yeast by decreased TOR pathway signaling. *Genes Dev.* **20**, 174–184 (2006).
9. D. E. Harrison, R. Strong, Z. D. Sharp, J. F. Nelson, C. M. Astle, K. Flurkey, N. L. Nadon, J. E. Wilkinson, K. Frenkel, C. S. Carter, M. Pahor, M. A. Javors, E. Fernandez, R. A. Miller, Rapamycin fed late in life extends lifespan in genetically heterogeneous mice. *Nature* **460**, 392–395 (2009).
10. N. D. Bonawitz, M. Chatenay-Lapointe, Y. Pan, G. S. Shadel, Reduced TOR signaling extends chronological life span via increased respiration and upregulation of mitochondrial gene expression. *Cell Metab.* **5**, 265–277 (2007).
11. M. Hansen, S. Taubert, D. Crawford, N. Libina, S. J. Lee, C. Kenyon, Lifespan extension by conditions that inhibit translation in *Caenorhabditis elegans*. *Aging Cell* **6**, 95–110 (2007).
12. C. K. Tsang, H. Qi, L. F. Liu, X. F. Zheng, Targeting mammalian target of rapamycin (mTOR) for health and diseases. *Drug Discov. Today* **12**, 112–124 (2007).
13. P. T. Bhaskar, N. Hay, The two TORCs and Akt. *Dev. Cell* **12**, 487–502 (2007).
14. D. A. Foster, A. Toschi, Targeting mTOR with rapamycin: One dose does not fit all. *Cell Cycle* **8**, 1026–1029 (2009).
15. S. Wullschleger, R. Loewith, M. N. Hall, TOR signaling in growth and metabolism. *Cell* **124**, 471–484 (2006).
16. D. C. Rubinsztein, The roles of intracellular protein-degradation pathways in neurodegeneration. *Nature* **443**, 780–786 (2006).

17. D. Zemke, S. Azhar, A. Majid, The mTOR pathway as a potential target for the development of therapies against neurological disease. *Drug News Perspect.* **20**, 495–499 (2007).
18. S. Sarkar, E. O. Perlstein, S. Imarisio, S. Pineau, A. Cordenier, R. L. Maglathlin, J. A. Webster, T. A. Lewis, C. J. O'Kane, S. L. Schreiber, D. C. Rubinsztein, Small molecules enhance autophagy and reduce toxicity in Huntington's disease models. *Nat. Chem. Biol.* **3**, 331–338 (2007).
19. B. C. Capell, M. R. Erdos, J. P. Madigan, J. J. Fiordalisi, R. Varga, K. N. Conneely, L. B. Gordon, C. J. Der, A. D. Cox, F. S. Collins, Inhibiting farnesylation of progerin prevents the characteristic nuclear blebbing of Hutchinson-Gilford progeria syndrome. *Proc. Natl. Acad. Sci. U.S.A.* **102**, 12879–12884 (2005).
20. B. Liu, Z. Zhou, Lamin A/C, laminopathies and premature ageing. *Histol. Histopathol.* **23**, 747–763 (2008).
21. B. Liu, J. Wang, K. M. Chan, W. M. Tjia, W. Deng, X. Guan, J. D. Huang, K. M. Li, P. Y. Chau, D. J. Chen, D. Pei, A. M. Pendas, J. Cadiñanos, C. López-Otín, H. F. Tse, C. Hutchison, J. Chen, Y. Cao, K. S. Cheah, K. Tryggvason, Z. Zhou, Genomic instability in laminopathy-based premature aging. *Nat. Med.* **11**, 780–785 (2005).
22. D. S. Evans, P. Kapahi, W. C. Hsueh, L. Kockel, TOR signaling never gets old: Aging, longevity and TORC1 activity. *Ageing Res. Rev.* **10**, 225–237 (2011).
23. Z. Berger, B. Ravikumar, F. M. Menzies, L. G. Oroz, B. R. Underwood, M. N. Pangalos, I. Schmitt, U. Wullner, B. O. Evert, C. J. O'Kane, D. C. Rubinsztein, Rapamycin alleviates toxicity of different aggregate-prone proteins. *Hum. Mol. Genet.* **15**, 433–442 (2006).
24. T. Pan, P. Rawal, Y. Wu, W. Xie, J. Jankovic, W. Le, Rapamycin protects against rotenone-induced apoptosis through autophagy induction. *Neuroscience* **164**, 541–551 (2009).
25. D. McClintock, D. Ratner, M. Lokuge, D. M. Owens, L. B. Gordon, F. S. Collins, K. Djabali, The mutant form of lamin A that causes Hutchinson-Gilford progeria is a biomarker of cellular aging in human skin. *PLoS One* **2**, e1269 (2007).
26. N. Mizushima, T. Noda, T. Yoshimori, Y. Tanaka, T. Ishii, M. D. George, D. J. Klionsky, M. Ohsumi, Y. Ohsumi, A protein conjugation system essential for autophagy. *Nature* **395**, 395–398 (1998).
27. N. Mizushima, H. Sugita, T. Yoshimori, Y. Ohsumi, A new protein conjugation system in human. The counterpart of the yeast Apg12p conjugation system essential for autophagy. *J. Biol. Chem.* **273**, 33889–33892 (1998).
28. P. O. Seglen, P. B. Gordon, 3-Methyladenine: Specific inhibitor of autophagic/lysosomal protein degradation in isolated rat hepatocytes. *Proc. Natl. Acad. Sci. U.S.A.* **79**, 1889–1892 (1982).
29. J. P. Belzile, J. Richard, N. Rougeau, Y. Xiao, E. A. Cohen, HIV-1 Vpr induces the K48-linked polyubiquitination and proteasomal degradation of target cellular proteins to activate ATR and promote $G_2$ arrest. *J. Virol.* **84**, 3320–3330 (2010).
30. I. Dikic, S. Wakatsuki, K. J. Walters, Ubiquitin-binding domains—from structures to functions. *Nat. Rev. Mol. Cell Biol.* **10**, 659–671 (2009).
31. J. M. Tan, E. S. Wong, V. L. Dawson, T. M. Dawson, K. L. Lim, Lysine 63-linked polyubiquitin potentially partners with p62 to promote the clearance of protein inclusions by autophagy. *Autophagy* **4**, 251–253 (2007).
32. J. M. Tan, E. S. Wong, D. S. Kirkpatrick, O. Pletnikova, H. S. Ko, S. P. Tay, M. W. Ho, J. Troncoso, S. P. Gygi, M. K. Lee, V. L. Dawson, T. M. Dawson, K. L. Lim, Lysine 63-linked ubiquitination promotes the formation and autophagic clearance of protein inclusions associated with neurodegenerative diseases. *Hum. Mol. Genet.* **17**, 431–439 (2008).
33. M. Komatsu, S. Waguri, M. Koike, Y. S. Sou, T. Ueno, T. Hara, N. Mizushima, J. Iwata, J. Ezaki, S. Murata, J. Hamazaki, Y. Nishito, S. Iemura, T. Natsume, T. Yanagawa, J. Uwayama, E. Warabi, H. Yoshida, T. Ishii, A. Kobayashi, M. Yamamoto, Z. Yue, Y. Uchiyama, E. Kominami, K. Tanaka, Homeostatic levels of p62 control cytoplasmic inclusion body formation in autophagy-deficient mice. *Cell* **131**, 1149–1163 (2007).
34. G. Bjørkøy, T. Lamark, A. Brech, H. Outzen, M. Perander, A. Overvatn, H. Stenmark, T. Johansen, p62/SQSTM1 forms protein aggregates degraded by autophagy and has a protective effect on huntingtin-induced cell death. *J. Cell Biol.* **171**, 603–614 (2005).
35. M. Filimonenko, P. Isakson, K. D. Finley, M. Anderson, H. Jeong, T. J. Melia, B. J. Bartlett, K. M. Myers, H. C. Birkeland, T. Lamark, D. Krainc, A. Brech, H. Stenmark, A. Simonsen, A. Yamamoto, The selective macroautophagic degradation of aggregated proteins requires the PI3P-binding protein Alfy. *Mol. Cell* **38**, 265–279 (2010).
36. B. Ravikumar, R. Duden, D. C. Rubinsztein, Aggregate-prone proteins with polyglutamine and polyalanine expansions are degraded by autophagy. *Hum. Mol. Genet.* **11**, 1107–1117 (2002).
37. D. A. Krueger, M. M. Care, K. Holland, K. Agricola, C. Tudor, P. Mangeshkar, K. A. Wilson, A. Byars, T. Sahmoud, D. N. Franz, Everolimus for subependymal giant-cell astrocytomas in tuberous sclerosis. *N. Engl. J. Med.* **363**, 1801–1811 (2010).
38. M. Olive, I. Harten, R. Mitchell, J. K. Beers, K. Djabali, K. Cao, M. R. Erdos, C. Blair, B. Funke, L. Smoot, M. Gerhard-Herman, J. T. Machan, R. Kutys, R. Virmani, F. S. Collins, T. N. Wight, E. G. Nabel, L. B. Gordon, Cardiovascular pathology in Hutchinson-Gilford progeria: Correlation with the vascular pathology of aging. *Arterioscler. Thromb. Vasc. Biol.* **30**, 2301–2309 (2010).
39. **Acknowledgments:** We thank S. Wincovitch and A. Dutra for support of the quantitative progerin intensity experiments, S. Anderson for support with FACS analysis, M. Olive and E. Nabel for informative discussion, and A. Yamamoto for the p62 and ALFY constructs. **Funding:** This work was supported by grants R00AG029761 (K.C.) and R01NS051303 (D.K.), The Progeria Research Foundation (J.J.G. and D.K.), and the intramural program of the National Human Genome Research Institute (F.S.C.). **Competing interests:** The authors declare that they have no competing interests.

Submitted 3 March 2011
Accepted 2 June 2011
Published 29 June 2011
10.1126/scitranslmed.3002346

**Citation:** K. Cao, J. J. Graziotto, C. D. Blair, J. R. Mazzulli, M. R. Erdos, D. Krainc, F. S. Collins, Rapamycin reverses cellular phenotypes and enhances mutant protein clearance in Hutchinson-Gilford progeria syndrome cells. *Sci. Transl. Med.* **3**, 89ra58 (2011).